Interactive CardioVascular and Thoracic Surgery 2022, 35(4), ivac227
https://doi.org/10.1093/icvts/ivac227 Advance Access publication 6 September 2022

ORIGINAL ARTICLE

EXPERIMENTAL

Cite this article as: Carlson Hanse L, Tjørnild MJ, Sørensen SG, Johansen P, Lugones I, Hjortdal VE. Trileaflet semilunar valve reconstruction: pulsatile *in vitro* evaluation. Interact CardioVasc Thorac Surg 2022; doi:10.1093/icvts/ivac227.

Trileaflet semilunar valve reconstruction: pulsatile *in vitro* evaluation

Lisa Carlson Hanse [a,b,*], Marcell J. Tjørnild [a,b], Simon G. Sørensen[b,c], Peter Johansen[d], Ignacio Lugones[e] and Vibeke E. Hjortdal[f]

[a] Department of Cardiothoracic and Vascular Surgery, Aarhus University Hospital, Aarhus, Denmark
[b] Department of Clinical Medicine, Aarhus University Hospital, Aarhus, Denmark
[c] Department of Molecular Medicine (MOMA), Aarhus University Hospital, Aarhus, Denmark
[d] Department of Engineering, Aarhus University, Aarhus, Denmark
[e] Department of Congenital Heart Surgery in Hospital General de Niños "Pedro de Elizalde", Buenos Aires, Argentina
[f] Department of Cardiothoracic Surgery, Rigshospitalet, Copenhagen, Denmark

* Corresponding author. Department of Cardiothoracic & Vascular Surgery, Aarhus University Hospital, Skejby, Palle Juul-Jensens Boulevard 99, 8200 Aarhus, Denmark. Tel: +45-78-45-30-80; fax: +45-78-45-30-79; e-mail: carlson.hanse@clin.au.dk (L. Carlson Hanse).

Received 16 April 2022; received in revised form 11 July 2022; accepted 5 September 2022

Key question

Is trileaflet semilunar valve reconstruction (TSVR) achievable as a functional pulmonary valve reconstruction *in vitro*?

Key finding(s)

TSVR: is sufficient; is non-stenotic; have an increased coaptation; have a windmill shape; mimic native leaflet motions.

Take-home message

New surgical technique for pulmonary valve reconstruction with findings speculated to accommodate for growth with the patient.

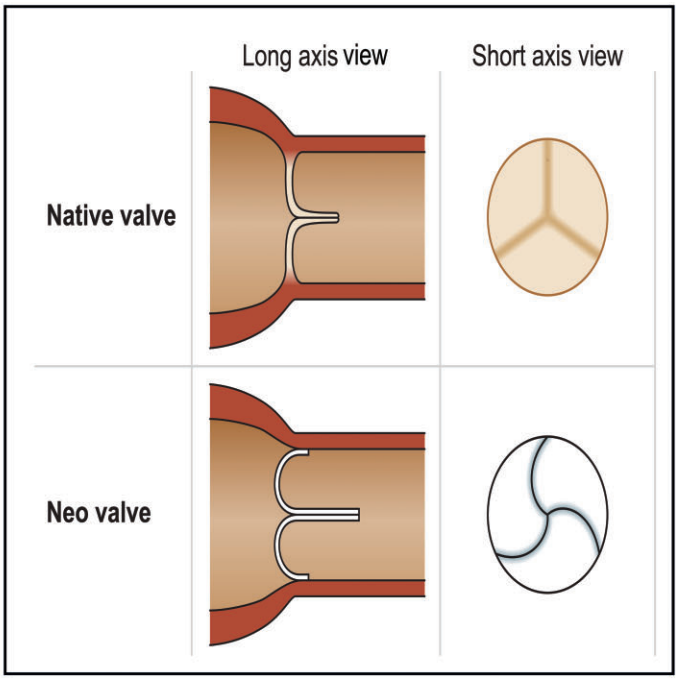

Abstract

OBJECTIVES: Residual regurgitation is common after congenital surgery for right ventricular outflow tract malformation. It is accepted as there is no competent valve solution in a growing child. We investigated a new surgical technique of trileaflet semilunar valve reconstruction possessing the potential of remaining sufficient and allowing for some growth with the child. In this proof-of-concept study, our aim was to evaluate if it is achievable as a functional pulmonary valve reconstruction *in vitro*.

METHODS: Explanted pulmonary trunks from porcine hearts were evaluated in a pulsatile flow-loop model. First, the native pulmonary trunk was investigated, after which the native leaflets were explanted. Then, trileaflet semilunar valve reconstruction was performed and investigated. All valves were initially investigated at a flow output of 4 l/min and subsequently at 7 l/min. The characterization was based on hydrodynamic pressure and echocardiographic measurements.

RESULTS: Eight pulmonary trunks were evaluated. All valves are competent on colour Doppler. There is no difference in mean pulmonary systolic artery pressure gradient at 4 l/min ($P = 0.32$) and at 7 l/min ($P = 0.20$). Coaptation length is increased in the neo-valve at 4 l/min ($P < 0.001$, $P < 0.001$, $P = 0.008$) and at 7 l/min ($P < 0.001$, $P = 0.006$, $P = 0.006$). A windmill shape is observed in all neo-valves.

CONCLUSIONS: Trileaflet semilunar valve reconstruction is sufficient and non-stenotic. It resulted in an increased coaptation length and a windmill shape, which is speculated to decrease with the growth of the patient, yet remains sufficient as a transitional procedure until a long-term solution is feasible. Further *in vivo* investigations are warranted.

Keywords: TSVR • Neo-valve • Pulmonary valve reconstruction • Congenital • *In vitro*

ABBREVIATIONS

AC	Anterior cusp
LC	Left cusp
RC	Right cusp
RVOT	Right ventricular outflow tract
STJ	Sinotubular junction
TOST	Two one-sided test
TSVR	Trileaflet semilunar valve reconstruction
ePTFE	Expandable Polytetrafluoreten

INTRODUCTION

Right ventricular outflow tract (RVOT) malformations are present in an estimated 20% of children with congenital heart disease [1], including tetralogy of Fallot, pulmonary valve disease or pulmonary atresia. A significant proportion of these children require multiple surgical or catheter-based interventions in childhood. These interventions are often transitional—in the wait for timely pulmonary valve replacement later in life—and leave the pulmonary valve with anatomic and functional abnormalities. The subsequent residual pulmonary regurgitation can be well tolerated for decades; however, complications such as arrhythmias, right ventricular heart failure and sudden cardiac death may occur, sometimes at very young age [2]. These complications cause an ongoing search for determining the optimal time for re-valving and the optimal valve that will suit the growing child.

Trileaflet semilunar valve reconstruction (TSVR) is a new surgical technique, created by Dr. Lugones, in which the leaflets in a native semilunar valve are replaced with customized semilunar leaflet patches. This article is the first in a series of 3 studies investigating this novel surgical technique going from *in vitro*, over to an animal model and then to a final human testing. In this proof-of-concept study, we are investigating the achievability of TSVR on the pulmonary valve *in vitro* in a pulsatile model. The characterization is based on hydrodynamic and geometric properties measured by pressure catheters and echocardiography.

MATERIALS AND METHODS

Porcine pulmonary trunks

We explanted pulmonary trunks from 9 porcine hearts, obtained fresh from 90-kg pigs at a local abattoir. The pulmonary trunks were harvested using the Ross technique. They were trimmed to incorporate 1 cm of the RVOT and 3 cm of the common pulmonary artery.

Only pulmonary trunks with a trileaflet pulmonary valve, symmetric sinuses of Valsalva and no macroscopic pathology were included. One was excluded due to a bicuspid pulmonary valve.

Leaflet patches

For the leaflet patches, porcine pericardium was obtained fresh from a second abattoir and treated with glutaraldehyde. First, the pericardium was rinsed of excess tissue, and then, it was suspended onto polystyrene and submerged into a glutaraldehyde 0.6% solution for 15 min. It was subsequently rinsed in saline water and stored submerged in 0.01 M, 7.4 pH, phosphate buffer at 4°C. After 24 h in the phosphate buffer, the buffer was replaced with fresh 0.01 M, 7.4 pH, phosphate buffer and the pericardium was continuously stored submerged at 4°C. Prior to implantation, the treated pericardium was rinsed in saline water and the leaflet patches were cut out using a custom template.

The size of the leaflet patches was determined based on the diameter of the sinotubular junction (STJ) by echocardiography when the native pulmonary trunk was suspended in a right heart simulator and subjected to a flow of 7 l/min. Each neo-valve was reconstructed using 3 identical leaflet patches. The degree of oversizing is based on the logarithmic growth of the pulmonary valve annulus and the main pulmonary artery [3], determined by the initial diameter of these structures and the expected growth velocity. Theoretically, the degree of oversizing will be greater in smaller patients, who exhibit increased growth velocity, to ensure valve competence over a longer time period.

Ethics statement

Biological tissue was obtained from 2 distinct abattoirs. Application for the approval of this study was not required.

Right heart simulator

We used a pulsatile simulator of the right side of the heart, which mimics a beating heart in terms of flow and pressure. This machine has previously been used for biomechanical studies of semilunar valves in the aortic [4] and the pulmonary [5] positions. The simulator consisted of: an atrial chamber; a ventricular chamber; and a compliance chamber (Fig. 1). The atrial chamber and the ventricular chamber were separated by a mechanical valve. The compliance chamber was connected to the atrial chamber through an elastic tube. Pulsatile flow was produced by a Series piston pump (SuperPump AR; ViVitro Labs, Victoria, Canada), connected to the ventricular chamber. Both the ventricular chamber and the compliance chamber had respective insertions ports for pressure catheters and respective sites of attachment for customized pulmonary trunk holders.

The customized pulmonary trunk holders were developed in 2 different sizes, as the pulmonary trunk has a cone shape with the broadest base at the right ventricular infundibulum and the most narrow part at the common pulmonary artery. The holders were made of expanded Polytetrafluoreten (ePTFE) vascular grafts

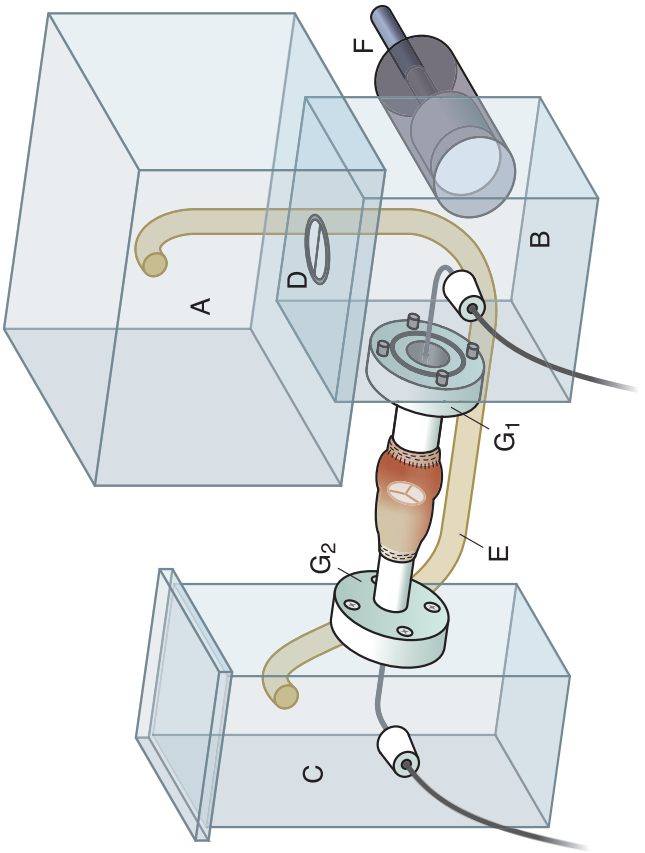

Figure 1: Illustration of the right heart simulator: (**A**) atrial chamber; (**B**) ventricular chamber; (**C**) compliance chamber; (**D**) mechanical valve; (**E**) recirculation tube; (**F**) piston pump; (**G_1**) pulmonary trunk holder, ventricular; and (**G_2**) pulmonary trunk holder, main pulmonary artery.

tubing (GORE-TEX®; W.L. Gore & Associates, Flagstaff, AZ, USA). Sizing of the ePTFE vascular grafts was determined based on measurements from 8 explanted porcine pulmonary trunks. The ventricular diameter was manually measured 1 cm below the annulus and the pulmonary artery diameter was manually measured 3 cm above the annulus. Based on these measurements, the ventricular holder resulted in a diameter of 24 mm and the common pulmonary artery holder resulted in a diameter of 16 mm. On each end of the pulmonary trunk holders, a tube of polyethylene terephthalate fabric (Dacron®; Dupont, Wilmington, DE, USA) was attached.

Mounting of the pulmonary trunk

The pulmonary trunks were sutured onto the polyethylene terephthalate fabric lining of their respective pulmonary trunk holder with continuous suture using 5–0 Prolene® (Ethicon, Somerville, NJ, USA). The pulmonary trunk was subsequently mounted between the ventricular chamber and the compliance chamber on the simulator.

Flow and imaging modalities

For ventricular and pulmonary flow, an ultrasonic transit time flow system (PXL11, PXL25, TS410; Transonic Systems Inc., Ithaca, USA) was used. For right ventricular and pulmonary pressure measurements, micro-tip pressure catheters (SPR-350S; Millar Instruments, Houston, TX, USA) were used and amplified with a two-channel pressure control unit (PCU-2000; Millar Instruments). The pressure sensors were calibrated and zeroed prior to each experiment.

For echocardiographic measurements, a 2D-linear probe (GE 9l-RS Probe; GE Healthcare, Horten, Norway) was used on the pulmonary trunk. Images were obtained in a short-axis view at the level of the sinuses and in long-axis views projecting through each of the 3 commissures. The leaflets of the valves will be referred to as the anterior cusp (AC), right cusp (RC) and left cusp (LC) and the 3 long-axis echocardiographic views as LC–AC, AC–RC and RC–LC.

Study design

This is an *in vitro* experimental study. The pulmonary trunks were investigated before and after TSVR with customized leaflet patches in a pulsatile flow simulator of the right side of the heart. Each pulmonary trunk served as its own control.

Experimental setup

The valves were first investigated at a flow output of 4 l/min. After complete data acquisition, the valves were investigated again at a flow output to 7 l/min. The flow output was generated by increasing the stroke volume of the piston pump, which dispatched water in the ventricular chamber through the pulmonary trunk. These 2 flow outputs were used as a measure for cardiac output at 'rest' and at 'exercise'.

Three customized leaflet patches were cut out (Fig. 2A). After the complete acquisition of data from the native pulmonary trunk, the native pulmonary leaflets were excised at the level of attachment to the pulmonary artery wall (Fig. 2B), through a longitudinal incision on the anterior aspect of the main pulmonary artery. We had an insertion template sized after the STJ measurement, which in this study was only used to confirm the symmetry of the native valve characterized by 3 leaflets of the same size. The pulmonary leaflet patch was then sutured with 3 6–0 Prolene® suture loops to the mid-point of the line of attachment (nadir) of the native leaflet (Fig. 2C) and subsequently parachuted down (Fig. 2D). Then, 1 side of the pulmonary leaflet patch was attached to the pulmonary trunk. The continuous suture followed the line of native attachment, as the valves were symmetric. Care was taken not to perforate the pulmonary artery wall (Fig. 2E). Prior to the zone of apposition with the adjacent leaflets, we created a reinforcement area. This reinforcement area was sutured with a horizontal mattress suture technique, resulting in the margin of the leaflet bulging into the lumen, that is, into the sinus of Valsalva (Fig. 2F). As the leaflet patches are oversized to accommodate growth, their free margin ends a few millimetres above the native free margin. Once the neo-leaflet was attached, the needles on both ends of the suture perforated the pulmonary wall from the inside to the outside at the level of the new free margin (Fig. 2G). The 2 other pericardial leaflets were attached in a similar fashion. Once all 3 leaflets had been attached to the native pulmonary trunk, a securing suture attached the neighbouring leaflet borders to each other. The securing suture was going from the outside through the pulmonary artery wall at the level of the new commissure (Fig. 2H), through the reinforcement area, through the leaflet, through the neighbouring leaflet,

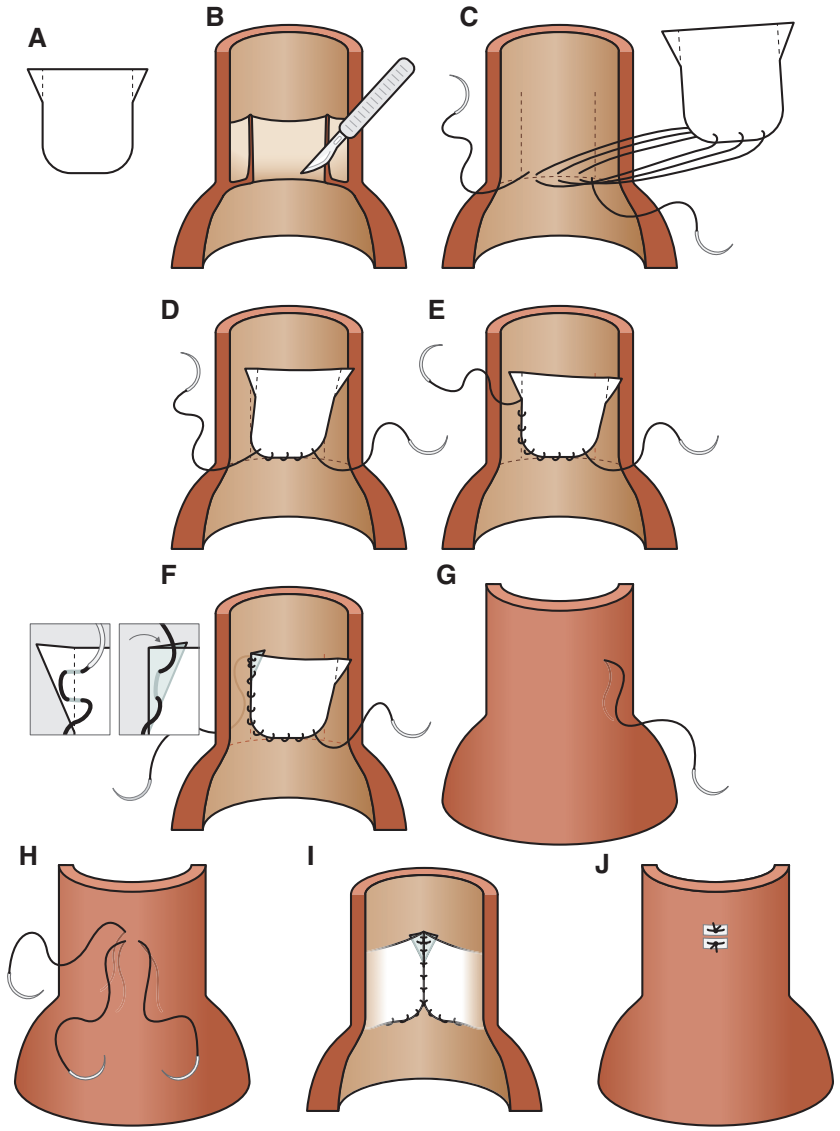

Figure 2: Illustration of the surgical technique used for replacing the native pulmonary cusps with oversized pericardial cusp patches. (**A**) The oversized cusp patch. Striped lines: the reinforcement areas; (**B**) excision of the native pulmonary cusps; (**C**) attachment of the oversized pericardial cusp patch to the base of the annulus using 3 suture loops; dotted line: annulus; (**D**) parachuting of the leaflet to the base of the annulus; (**E**) attachment of 1 side of the leaflet to the annulus with continuous suture; (**F**) attachment of the reinforcement area on the leaflet with horizontal mattresses; (**G**) penetration of the suture through the pulmonary artery at the level of the leaflet; securing suture from the (**H**) outside and (**I**) inside; and (**J**) attachment with felt pledgets.

through the neighbouring reinforcement area and out at the same level (Fig. 2I). Felt pledgets were placed to secure the sutures on the outer surface of the pulmonary artery. The neighbouring leaflet sutures were tied down together, and the securing sutures were tied down together (Fig. 2J).

Data acquisition and data analysis

Data were acquired for each level of flow output by the same person and in the same laboratory, using the same equipment.

Pressure and flow data were recorded using dedicated data acquisition hardware (NI-9215; National Instruments, Austin, TX, USA) for 10 consecutive cycles at a sampling rate of 1000 Hz. It was stored and analysed offline using LabVIEW 11.0 (National Instruments). The systolic and diastolic pressures were determined as maximum and minimum pressures for the right ventricle and the pulmonary valve, respectively. Systolic gradient is calculated from start systole to end systole. Diastolic gradient is calculated as the difference in pressure from 15% onto the pressure timeline from end systole to end diastole. The 15% was added to the systolic pressure to let the ventricle pressure fall to the diastolic level due to pressure probe placement.

Echocardiographic data were stored and analysed offline using EchoPac 113.0.4 (GE Healthcare, Horten, Norway). The echocardiographic systole and diastole were visually defined when the annular diameter was respectively at the maximum and minimum lengths [4]. The acquired parameters in the short-axis view were: geometric orifice area; planimetric cross-sectional sinus area (systole, diastole), and in the long-axis view: annular base internal diameter (systole, diastole); STJ internal diameter (systole and diastole); coaptation length; and billow (a positive value above the annular plane and a negative value below the annular plane). The hydrodynamic assessment was performed using colour Doppler, where competence was defined as the absence of a

diastolic jet. The parameters reported were calculated using standard built-in functions in EchoPac.

Statistical analysis

All parameters are reported as mean ± standard deviation. Hydrodynamic flow and pressure parameters were based on 10 consecutive cardiac cycles, and a mean was calculated for each parameter across these cycles. Echocardiographic parameters were measured manually at a single timepoint. For each parameter, normal distribution of the data was evaluated using QQ plots.

Means before and after intervention were compared. To test for significant difference between means, a paired two-tailed Student's *t*-test was applied. If the H_0 hypothesis of no difference was accepted, a two one-sided test (TOST) was used to determine whether the means were equivalent with a predefined difference ε defined as the mean standard deviation of measurements before and after interventions:

$$\varepsilon = \frac{\sigma_{\text{before}} + \sigma_{\text{after}}}{2}.$$

This value of ε is defined as such, to discover parameters with a high level of equivalence relative to the uncertainty of the measurements.

P-Values are reported for the two-tailed Student's *t*-test unless other is specified. *P*-Values of both the two-tailed Student's *t*-test and the TOST were corrected for multiple testing to reach a false discovery rate of 0.05, and *q*-values below 0.05 were considered significant. All statistical analyses were performed using R version 4.0.2 (R Foundation for Statistical Computing, Vienna, Austria) and the package Equivalence version 0.7.2.

RESULTS

Eight pulmonary trunks were investigated. Baseline *in vitro* hydrodynamics are presented in Table 1. The trunks were investigated under similar conditions. The internal diameter for the STJ was: 4 trunks: 31 mm; 1 trunk: 33 mm; 2 trunks: 35 mm; and 1 trunk: 36 mm. No structural damage to the customized pulmonary leaflet patches after TSVR was observed at both flow outputs of 4 and 7 l/min.

Pressure

At 4 l/min, there was no difference and equivalence in: mean pulmonary artery systolic pressure gradient (TOST, $P = 0.019$; Fig. 3A) and mean pulmonary artery diastolic pressure gradient (TOST, $P = 0.045$; Fig. 3B). At 7 l/min, there was no difference and equivalence in: mean pulmonary artery systolic pressure gradient (TOST, $P = 0.11$; Fig. 3A) and mean pulmonary artery diastolic pressure gradient (TOST, $P = 0.095$; Fig. 3B).

Echocardiography

Short-axis view. All valves presented with a windmill shape. The geometric orifice area was not different and not equivalent for the neo-valve at 4 l/min (TOST, $P = 0.10$) and 7 l/min (TOST, $P = 0.065$) (Fig. 4A). The planimetric cross-sectional sinus area decreased in the neo-valve in systole and diastole and at both flow outputs (Fig. 4B).

Table 1: *In vitro* hydrodynamics

Variable	4 l/min	7 l/min
$Flow_{max}$ (l/min)		
Native	3.9 ± 0.2	7.3 ± 0.2
Neo-valve	3.9 ± 0.2	7.3 ± 0.2
$Flow_{min}$ (l/min)		
Native	1.9 ± 0.2	4.0 ± 0.2
Neo-valve	1.9 ± 0.2	3.9 ± 0.5
RVSP (mmHg)		
Native	29.0 ± 1.8	48.6 ± 1.8
Neo-valve	28.9 ± 1.1	48.0 ± 1.5
PASP (mmHg)		
Native	27.5 ± 2.4	47.2 ± 2.3
Neo-valve	27.4 ± 2.3	46.1 ± 2.5

Values are presented as mean ± SD.

$Flow_{max}$: maximum flow; $Flow_{min}$: minimum flow; PASP: pulmonary artery systolic pressure; RVSP: right ventricular systolic pressure; SD: standard deviation.

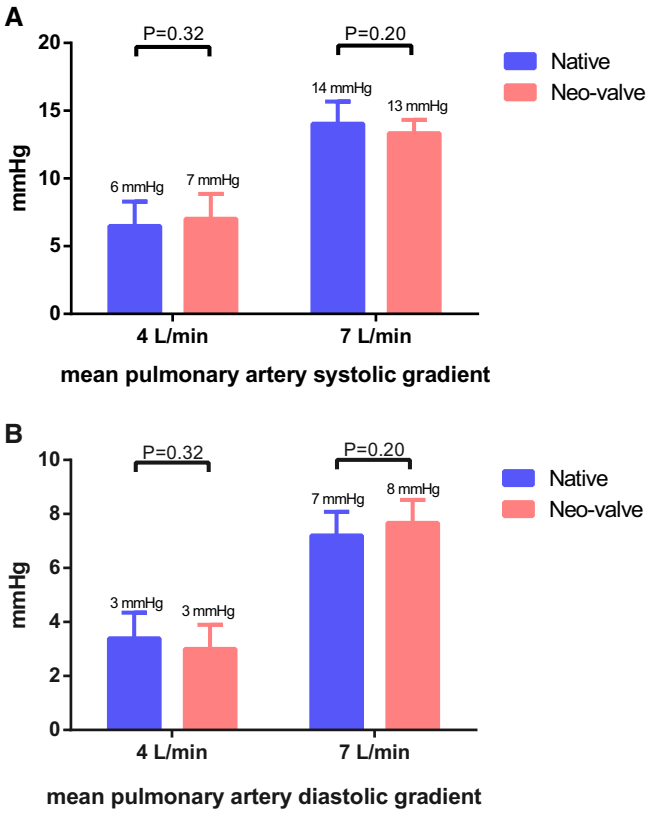

Figure 3: Grouped bars chart with mean and standard deviation at 4 and 7 l/min: (**A**) mean systolic pulmonary artery gradient and (**B**) mean diastolic pulmonary artery gradient.

Long-axis view. At both flow outputs, the native valves and the neo-valves were functional, with absent diastolic jets on colour Doppler in the long-axis views.

Coaptation length in all 3 echocardiographic views (LC–AC, AC–RC and RC–LC), increased in the neo-valve both at 4 l/min ($P < 0.001$, $P < 0.001$, $P = 0.008$) and at 7 l/min ($P < 0.001$, $P = 0.006$, $P = 0.006$) (Fig. 5A). All leaflets in the neo-valve billow below the annular plane at both flow outputs (Fig. 5B).

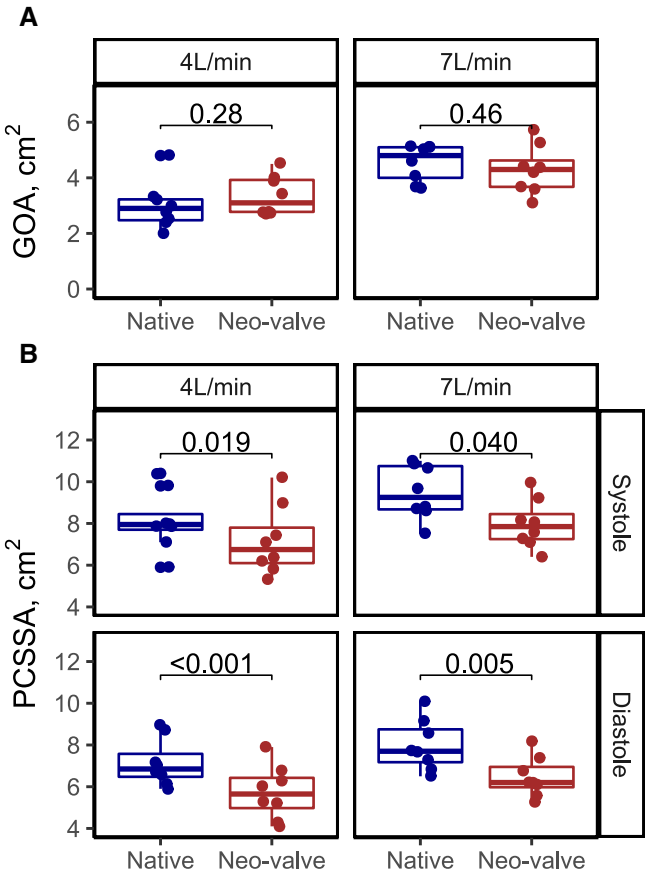

Figure 4: Box plots and whiskers with median and upper/lower interquartile range × 1.5 depicting (**A**) GOA and (**B**) PCSSA for the native valve and neo-valve in both systole and diastole at 4 and 7 l/min, respectively. GOA: geometric orifice area; PCSSA: planimetric cross-sectional sinus area.

The diameter of the annulus in all 3 echocardiographic views was not different. It was not equivalent in systole at both 4 and 7 l/min in all 3 echocardiographic views (Fig. 6A). In diastole, it was only equivalent at 4 l/min in the AC–RC view (TOST, $P < 0.001$) and at 6 l/min in the AC–RC (TOST, $P = 0.037$) and RC–LC (TOST, $P = 0.049$) views (Fig. 6B).

DISCUSSION

In children with RVOT malformations, i.e. pulmonary stenosis, pulmonary atresia and tetralogy of Fallot, transitional treatment causing residual regurgitation is often performed prior to pulmonary valve replacement. Pulmonary regurgitation results in chronic volume overload in the right ventricle, which can lead to exercise intolerance, progressive right ventricular dilatation, ventricular and atrial tachycardia, congestive heart failure and sudden cardiac death [2]. These adverse effects call for timely pulmonary valve intervention [6]. The main important findings in this study investigating TSVR on the pulmonary valve in a pulsatile flow-loop model are: (i) a sufficient neo-valve; (ii) a non-stenotic neo-valve; (iii) an increased coaptation length in the neo-valve; (iv) a windmill shape in the neo-valve; (v) and the leaflets in the neo-valve seem to mimic the motions of the native pulmonary valve.

To circumvent residual pulmonary regurgitation and to accommodate growth with the child in transitional treatments, there are a number of expandable valve conduits being investigated [7–9]. A technique of replacing the aortic valve leaflets, which is developed for the adult population [10] and has been performed on the pulmonary valve in adults [11], has recently been described in the paediatric population with isolated congenital aortic valve disorders [12]. Sizing of the neo-leaflets in this technique is based on the intercommissural distance, making it dependent on the native valve morphology and symmetry. The neo-leaflets are sutured following the native commissural lines of insertion. Therefore, a native valve with 3 leaflets of different size will result in a new valve that is asymmetric. This method could be particularly problematic in the paediatric population, in which bicuspid or dome-shaped malformations of the pulmonary valve are more common. Thus, in a bicuspid valve, a leaflet-by-leaflet replacement based on the intercommissural distance would result in a new bicuspid valve. Besides, developed for the adult population, this technique does not account for somatic growth.

The surgical technique of TSVR is developed specifically for the congenital population. Sizing of the customized leaflets is based on the diameter of the STJ, which corresponds to the level of the free margins of the leaflets. This results in a valve with 3 symmetrical sinuses of Valsalva and 3 neo-leaflets identical in shape and size. In diastole, this causes the midpoint of the free margin of each neo-leaflet to approach the centre. To achieve this in asymmetrical valves, the neo-leaflets are reconstructed on new insertion lines drawn inside the pulmonary root with a dedicated template.

Our study revealed a sufficient neo-valve after TSVR on colour Doppler and on mean pulmonary artery diastolic pressure gradient at both flow outputs. A competent pulmonary valve should minimize dilation of the right ventricle, the otherwise observed effect of pulmonary valve regurgitation when the right ventricle is adjusting for the increased stroke volume [13]. A competent valve in a growing child would delay or even prevent the development of related symptoms.

The neo-valve displayed no functional nor geometrical stenosis reflected by mean pulmonary artery systolic gradient and geometric orifice area at both flow outputs. In the clinic, pulmonary valve stenosis is diagnosed by determining the pressure gradient across the valve using echocardiography. Peak gradient should be below 36 mmHg for mild stenosis. Postponing many early interventions in the young could allow for enough somatic growth with the consequent possibility of either percutaneous or a mechanical pulmonary valve replacement.

The coaptation length was increased and all 3 leaflets billowed below the annular plane in all 3 echocardiographic views after TSVR. The neo-leaflets have a shape mimicking the shape of native leaflets in semilunar valves and are wider and longer than what has been published on the aortic valve [12]. The windmill shape seen in the short-axis view (Fig. 7A) and the billowing seen in the long-axis view (Fig. 7B) are desirable, particularly in the younger patients, to accommodate growth. In aortic literature, billowing below the annular plane is described as a type C coaptation and has been associated with the risk of mid-term repair failure [14]. On the contrary, increased coaptation length is a strong predictor for aortic valve durability [15]. We anticipate that as the child grows and the diameters of the annulus and STJ increase, the increased coaptation length will become shorter, yet remain sufficient and the billowed leaflets will move towards the annular plane.

The annulus was unaffected by the surgical technique, which is desirable in RVOT malformations. It did however decrease the

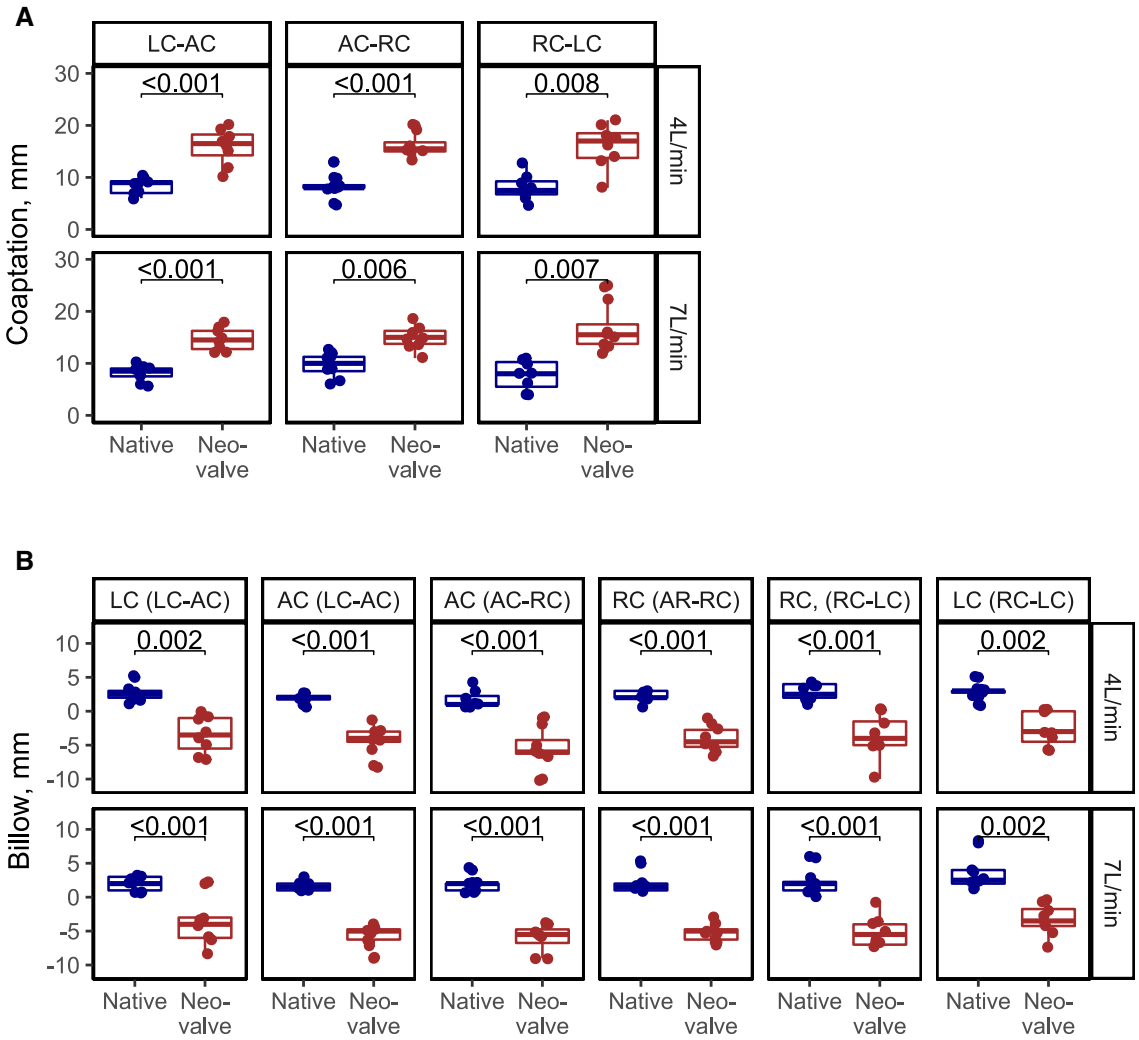

Figure 5: Box plots and whiskers with median and upper/lower interquartile range × 1.5 depicting (**A**) coaptation in all 3 echocardiographic views and (**B**) billow for each leaflet in all 3 echocardiographic views the native valve and neo-valve at 4 and 7 l/min, respectively.

diameter of the STJ, probably due to the closure of the pulmonary artery access. As it did not affect other parameters concluding competence and stenosis, the small decrease is regarded as unimportant.

Children are rarely at rest and testing a valve during higher flow rate comparable to a more active life is important. We tested the valve at 4 and 7 l/min corresponding to rest and moderate activity. During increased cardiac output in both healthy and diseased individuals, there is a disproportionate increase in afterload and wall stress on the right ventricle during exercise than that on the left ventricle [16]. The function of the neo-valve was unaltered during increased flow output from 4 to 7 l/min. As our neo-valve is competent and non-stenotic at both 'rest' and 'exercise', there is a reduced clinical concern of right ventricular deterioration.

The customized leaflets in this study are made of homologous glutaraldehyde treated porcine pericardium, due to logistical constraints. There is an ongoing debate on whether to use glutaraldehyde treatment or not. While glutaraldehyde makes pericardium easier to handle, it predisposes increased calcification rate in young patients [17]. Untreated pericardium is anti-immunogenic and seems to have histological benefits, serving as a scaffold for recellularization [18]. But it has been observed to shrink over time [19]. Consequently, there is a search for the perfect reconstruction material. Such a material should be biocompatible, strong and flexible to withstand the pressure changes during the cardiac cycle. It should furthermore not calcify, be anti-thrombogenic and possess tissue remodelling properties. Until we have the optimal material for cardiac surgery, we argue that fresh pericardium should be the preferred choice, especially under lower pressure conditions.

The neo-leaflets are oversized compared to the native normal size. Altered anatomy in aortic literature causes the leaflets to be subjected to increased force and stress [20]. The altered coaptation length and billow of the leaflets will further contribute to the altered dynamic on the leaflets. This will not be a concern as long as the pericardium and the suture are stronger than the forces and stresses subjected to the customized leaflets. Importantly, the low forces and stresses in this study proved sufficient for a functioning neo-valve.

During the past 2 decades, treatment of children with RVOT malformations has improved survival and quality of life. These advancements are dependent on the economic development of a country [21], why progress mainly benefit children in the developed world. Having an accessible surgical technique, which

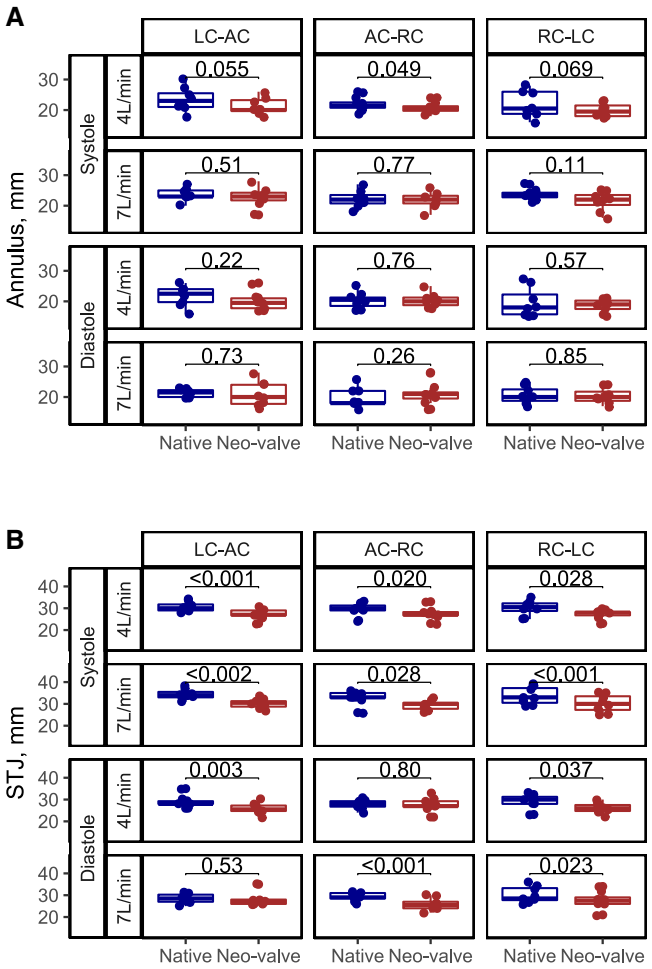

Figure 6: Box plots and whiskers with median and upper/lower interquartile range × 1.5 depicting (**A**) the annulus and (**B**) the STJ for the native valve and neo-valve in both systole and diastole at 4 and 7 l/min, respectively. STJ: sinotubular junction.

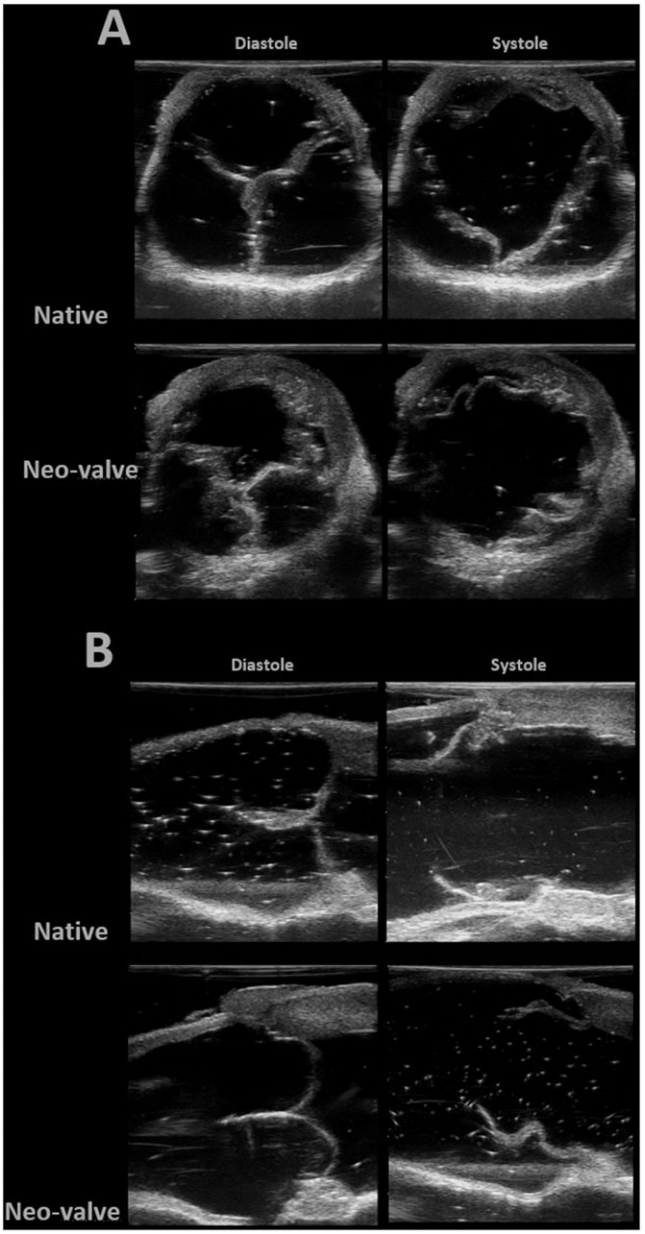

Figure 7: Echocardiographic images of the native and the neo-valve in (**A**) short-axis view and a (**B**) long-axis view.

achieve a competent valve and allows for some growth, in children where frequent follow-up can be challenging, could greatly benefit patients in developing countries. The customized design and the material used make TSVR both patient centred and economical.

TSVR is a method that does more than replace parts of the native semilunar valve complex. It reconstructs the root to achieve a symmetric trileaflet valve designed to stay competent with the growth of the patient.

Limitations

In vitro testing of a new surgical technique is a good method for proof of concept, prior to animal and human testing. The results from our study demonstrate that it is feasible to perform TSVR by replacing the native pulmonary leaflets with customized pericardial leaflet patches. The neo-valve seems to mimic the motions of the native pulmonary valve, is competent and non-stenotic and we can therefore speculate that the physiological conditions of the right side of the heart should remain unaltered in an *in vivo* setting. It is important to note that this *in vitro* model does not reflect pathologies that usually alter the flow dynamics *in vivo* in patient-specific ways. Sizing of the customized leaflet for TSVR was based on available porcine hearts. It is therefore not sized to the congenital population in this study, and direct translation should be performed with caution.

The fluid used for the study was room temperature water, and not body temperature blood. The difference in viscosity could affect fluid dynamics [22]. The model did not have eddy currents which are important for valve geometry and avoiding thrombosis formation *in vivo*. The increase in flow output was generated by increasing the stroke volume with no compensatory increase in frequency, making the piston pump forcefully push water throughout the *in vitro* setup at higher flow. Although the pulsatile flow loop model can isolate a biomechanical effect and we could study the pulmonary trunk from 3 angles with echocardiography, the model is a simplification of the complex interactions between the pulmonary valve and the right side of the

heart. This study does not provide mid-long-term results with respect to the durability of the valve.

CONCLUSION

TSVR was achievable *in vitro*. Hydrodynamic pressure and echocardiographic evaluations demonstrated a sufficient and non-stenotic neo-valve. The coaptation length increased, the leaflets billowed below the annular plane and we observed a windmill shape. We anticipate that as a child grows, the increased coaptation length will become shorter yet remain sufficient, the billowed leaflets will move towards the annular plane and the windmill shape will reduce. The results from this proof-of-concept study warrant further *in vivo* testing.

Funding

This work was supported by the Lundbeck Foundation [R184-2014-2478].

Conflict of interest: none declared.

Data availability

The data underlying this article will be shared on reasonable request to the corresponding author.

Author contributions

Lisa Carlson Hanse: Data curation; Formal analysis; Investigation; Project administration; Writing—review & editing. **Marcell J. Tjørnild:** Conceptualization; Investigation; Supervision; Writing—review & editing. **Simon G. Sørensen:** Data curation; Formal analysis; Software; Writing—review & editing. **Peter Johansen:** Conceptualization; Methodology; Supervision; Writing—review & editing. **Ignacio Lugones:** Conceptualization; Data curation; Investigation; Resources; Supervision; Writing—review & editing. **Vibeke E. Hjortdal:** Conceptualization; Formal analysis; Methodology; Resources; Supervision; Writing—review & editing.

Reviewer information

Interactive CardioVascular and Thoracic Surgery thanks Roman Gottardi and the other, anonymous reviewer(s) for their contribution to the peer review process of this article.

REFERENCES

[1] Bashore TM. Adult congenital heart disease: right ventricular outflow tract lesions. Circulation 2007;115:1933–47.
[2] Ammash NM, Dearani JA, Burkhart HM, Connolly HM. Pulmonary regurgitation after tetralogy of fallot repair: clinical features, sequelae, and timing of pulmonary valve replacement. Congenit Heart Dis 2007;2:386–403.
[3] Pettersen MD, Du W, Skeens ME, Humes RA. Regression equations for calculation of *Z* scores of cardiac structures in a large cohort of healthy infants, children, and adolescents: an echocardiographic study. J Am Soc Echocardiogr 2008;21:922–34.
[4] Sharghbin M, Benhassen LL, Lading T, Bechsgaard T, Skov SN, Røpcke DM *et al.* Comparison of the Dacron ring and suture annuloplasty for aortic root repair: an *in vitro* evaluation. Interact CardioVasc Thorac Surg 2018;27:819–27.
[5] Rasmussen J, Skov SN, Nielsen DB, Jensen IL, Tjørnild MJ, Johansen P *et al. in vitro* and *in vivo* evaluation of a novel bioprosthetic pulmonary valve for use in congenital heart surgery. J Cardiothorac Surg 2019;14:6–
[6] Kanter KR, Budde JM, Parks WJ, Tam VKH, Sharma S, Williams WH *et al.* One hundred pulmonary valve replacements in children after relief of right ventricular outflow tract obstruction. Ann Thorac Surg 2002;73:1801–7.
[7] Nunn GR, Bennetts J, Onikul E. Durability of hand-sewn valves in the right ventricular outlet. J Thorac Cardiovasc Surg 2008;136:290–6296.
[8] Russ JB, Li RL, Herschman AR, Waisman H, Vedula V, Kysar JW *et al.* Design optimization of a cardiovascular stent with application to a balloon expandable prosthetic heart valve. Mater Des 2021;209:109977.
[9] Hofferberth SC, Saeed MY, Tomholt L, Fernandes MC, Payne CJ, Price K *et al.* A geometrically adaptable heart valve replacement. Sci Transl Med 2020;12. https://doi.org/10.1126/scitranslmed.aay4006.A.
[10] Ozaki S, Kawase I, Yamashita H, Uchida S, Nozawa Y, Takatoh M *et al.* A total of 404 cases of aortic valve reconstruction with glutaraldehyde-treated autologous pericardium. J Thorac Cardiovasc Surg 2014;147:301–6.
[11] Yepez C, Rios J. Pulmonary valve reconstruction using Ozaki's technique for infective endocarditis. Eur J Cardiothorac Surg 2021;59:917–9.
[12] Wiggins LM, Mimic B, Issitt R, Ilic S, Bonello B, Marek J *et al.* The utility of aortic valve leaflet reconstruction techniques in children and young adults. J Thorac Cardiovasc Surg 2020;159:2369–78.
[13] Saji AM, Sharma S. Pulmonary Regurgiation, 2021. https://www.ncbi.nlm.nih.gov/books/NBK557564/ (24 February 2004, date last accessed).
[14] Pethig K, Milz A, Hagl C, Harringer W, Haverich A. Aortic valve reimplantation in ascending aortic aneurysm: risk factors for early valve failure. Ann Thorac Surg 2002;73:29–33.
[15] Bierbach BO, Aicher D, Issa OA, Bomberg H, Gräber S, Glombitza P *et al.* Aortic root and cusp configuration determine aortic valve function. Eur J Cardiothorac Surg 2010;38:400–6.
[16] La Gerche A, Rakhit DJ, Claessen G. Exercise and the right ventricle: a potential Achilles' heel. Cardiovasc Res 2017;113:1499–508.
[17] Schoen FJ, Levy RJ. Calcification of tissue heart valve substitutes: progress toward understanding and prevention. Ann Thorac Surg 2005;79:1072–80.
[18] Hibino N, Shin'oka T, Kurosawa H. Long-term histologic findings in pulmonary arteries reconstructed with autologous pericardium. N Engl J Med 2003;348:865–7.
[19] Pande S, Arya A, Agarwal SK, Tewari P, Kapoor A, Soni N *et al.* Long-term performance of untreated fresh autologous pericardium as a valve substitute in pulmonary position. Ann Card Anaesth 2022;25:164–70.
[20] Balachandran K, Sucosky P, Yoganathan AP. Hemodynamics and mechanobiology of aortic valve inflammation and calcification. Int J Inflam 2011;2011:263870–15.
[21] Zimmerman MS, Smith AGC, Sable CA, Echko MM, Wilner LB, Olsen HE *et al.* Global, regional, and national burden of congenital heart disease, 1990–2017: a systematic analysis for the Global Burden of Disease Study 2017. Lancet Child Adolesc Health 2020;4:185–200.
[22] Pohl M, Wendt MO, Werner S, Koch B, Lerche D. *in vitro* testing of artificial heart valves: comparison between Newtonian and Non-Newtonian fluids. Artif Organs 1996;20:37–46.